SCIENTIFIC REPORTS

OPEN

SUBJECT AREAS:
MATERIALS FOR ENERGY AND CATALYSIS
CHEMICAL PHYSICS

Received
1 August 2014

Accepted
7 November 2014

Published
28 November 2014

Correspondence and requests for materials should be addressed to Z.M. (zxmei@iphy.ac.cn) or X.D. (xldu@iphy.ac.cn)

Probing Defects in Nitrogen-Doped Cu_2O

Junqiang Li[1], Zengxia Mei[1], Lishu Liu[1], Huili Liang[1], Alexander Azarov[2], Andrej Kuznetsov[2], Yaoping Liu[1], Ailing Ji[3], Qingbo Meng[1] & Xiaolong Du[1]

[1]Key Laboratory for Renewable Energy, National Laboratory for Condensed Matter Physics, Institute of Physics, Chinese Academy of Sciences, P.O. Box 603, Beijing 100190, China, [2]Department of Physics, University of Oslo, P.O. Box 1048 Blindern, NO-0316 Oslo, Norway, [3]State Key Laboratory for Surface Physics, National Laboratory for Condensed Matter Physics, Institute of Physics, Chinese Academy of Sciences, P.O. Box 603, Beijing 100190, China.

Nitrogen doping is a promising method of engineering the electronic structure of a metal oxide to modify its optical and electrical properties; however, the doping effect strongly depends on the types of defects introduced. Herein, we report a comparative study of nitrogen-doping-induced defects in Cu_2O. Even in the lightly doped samples, a considerable number of nitrogen interstitials (N_i) formed, accompanied by nitrogen substitutions (N_O) and oxygen vacancies (V_O). In the course of high-temperature annealing, these N_i atoms interacted with V_O, resulting in an increase in N_O and decreases in N_i and V_O. The properties of the annealed sample were significantly modified as a result. Our results suggest that N_i is a significant defect type in nitrogen-doped Cu_2O.

Cuprous oxide (Cu_2O), a p-type semiconductor with a direct band gap of 2.1 eV, has long been considered a promising material for low-cost solar-energy conversion and photocatalysis[1–5]. Its advantages include a high absorption coefficient, a suitable band-gap width, chemical stability, non-toxicity and abundant reserves. Nitrogen doping in Cu_2O is an important research topic because of its tremendous potential for overcoming the major disadvantage of Cu_2O - its high resistance. Moreover, recent research has revealed that in addition to conductivity improvement, nitrogen-doped Cu_2O, hereafter referred to as Cu_2O:N, exhibits enhanced light absorption below the band gap, most likely because of the introduction of an intermediate band (IB) located ~0.7 eV above the valence band maximum (VBM)[6,7]. Its advantageous band gap and IB level have made Cu_2O:N an excellent candidate material for IB solar cells[8]. Its enhanced subband absorption in combination with its excellent visible-light absorption is also an outstanding advantage for photocatalysis because most inorganic photocatalysts suffer from poor activity or even inactivity under visible-light illumination, including the extensively studied TiO_2 and perovskite compounds[9–11]. However, several other groups have observed no enhancement in subband absorption even in heavily doped Cu_2O:N films[12,13], and Nakano et al. even observed a band-gap-widening effect upon nitrogen doping[14].

Through the application of first-principles calculations, several theoretical investigations of Cu_2O:N have also been performed. Li et al. claimed that nitrogen impurities in Cu_2O induce a marked widening of the band gap when oxygen vacancies are present[15], which could account for the experimentally observed optical band-gap widening of Cu_2O:N prepared via the sputtering technique[14]. Conversely, Zhao et al. reported a theoretical prediction that nitrogen doping should slightly widen the band gap, causing the formation of an IB in the gap located at ~0.9 eV above the VBM[16].

In general, there is still some controversy regarding the effects of nitrogen doping on Cu_2O, and no comprehensive understanding has yet been reached. It is well known that impurities at different sites in the lattice have distinct effects on the electrical and optical properties of a material[9,10]. However, interstitial nitrogen (N_i) in Cu_2O has long been ignored in previous experimental and theoretical studies, which have focused only on nitrogen impurities substituted at oxygen sites (N_O)[6,7,12,13,15–19]. In this work, we found that even in the lightly doped samples, a considerable number of N_i formed in Cu_2O, along with N_O and oxygen vacancies (V_O). In the course of annealing, migrating N_i reacted with V_O forming more N_O, thereby altering the corresponding contents of these point defects and resulting in a significant change of the optical and electrical properties of the material.

Results

Cu_2O and Cu_2O:N films were obtained via the post-oxidation of Cu (111) films that were initially deposited on c-plane Al_2O_3 buffered with a 400 nm thick, semi-insulating ZnO film[20]. Nitrogen doping was achieved by introducing a nitrogen plasma through a radio-frequency (RF) plasma gun during the oxidation process. It was found that a micro-zone phase separation occurs when fabricating Cu_2O films at high temperatures, while oxidizing at 300°C resulted in single oriented Cu_2O (111) films. So that this recipe was adopted for all samples used in this study. Figure 1(a) presents typical XRD θ-2θ scans for the samples. Only one peak corresponding to the Cu_2O (111) plane can be observed, in addition to the ZnO (0002) and Al_2O_3 (0006) signals; these results are consistent with the in situ reflection high-energy electron diffraction (RHEED) observations, as shown in Figure 1(b). Thus no traces of CuO, Cu or Cu_3N phases were found, suggesting high quality Cu_2O with diluted nitrogen in the doped samples. The clear RHEED patterns also indicate the fine crystallinity of the films. Atomic force microscopy images (not shown) revealed a uniform surface with a root-mean-square roughness of ~10 nm in a scan area of 10 μm × 10 μm.

The resistivities of the as-grown Cu_2O and Cu_2O:N samples were approximately 340 Ωcm and 100 Ωcm, respectively, measured by Hall effect. The carrier density and mobility of the Cu_2O were 3.5 × 10^{14} cm^{-3} and 53 $cm^2V^{-1}s^{-1}$, respectively. Interestingly, the Cu_2O:N sample demonstrated ambiguous p-type conduction behavior (Fig. S1 in the supplementary information), suggesting a low value for the Hall coefficient and/or the existence of hole traps. Annealing were applied to activate nitrogen related acceptors and/or remove the hole traps[17,19].

Figure 2(a) shows room temperature values for the hole density, mobility and resistivity of the Cu_2O and Cu_2O:N samples after annealing at 750°C for 10 min as functions of the nitrogen plasma power. A power of 0 W represents undoped Cu_2O. It is clear that the hole density increased with the power of the nitrogen plasma (likely to be proportional to the doping level) and the mobilities of Cu_2O:N were all smaller than those of Cu_2O (also consistent with the hypothesis of high nitrogen incorporation). The hole concentrations of Cu_2O:N were in the range of 10^{16} cm^{-3}, i.e. two orders of magnitude higher than that of Cu_2O[12,17–19]. Figure 2(b) presents the room temperature Hall data for Cu_2O:N synthesized using nitrogen plasma power of 200 W, as a function of annealing temperature. The lowest resistivity and the highest hole density were obtained upon annealing at 750°C. When the sample was annealed at 800°C, although the mobility was higher because of the improved crystal quality, the hole density decreased, leading to reduced conductivity. A possible explanation is that annealing at such a high temperature may also induce the out diffusion of nitrogen in addition to the acceptor activation. Note that the annealing conditions can be further optimized for better conductivity; nevertheless, in our study, the results indicated that the samples annealed at 750°C were already suitable for the study of nitrogen-related defects on behalf of the prominent evolution in electrical properties. Furthermore, the temperature-dependent hole concentration was also measured to determine the activation energy of the dominant acceptors in Cu_2O:N, which was calculated to be 121 meV (supplementary information). This level is attributed to extrinsic N_O acceptors, because the only reasonable alternative of copper vacancies (V_{Cu}) exhibits a much deeper level[21–23]. Figure 3 presents the nitrogen concentration versus depth profiles of the Cu_2O:N films doped with 200 W nitrogen plasma as measured by secondary ion mass spectroscopy (SIMS), which confirms: (i) nitrogen incorporation into our films and (ii) its gradual out diffusion during anneals.

Discussion

The data in Fig. 2 and Fig. 3 suggest that nitrogen, likely in favor of N_O, behaves as an efficient acceptor in Cu_2O:N. Logically, to enhance the conductivity of Cu_2O:N, we simply need to increase the doping level and/or optimize the annealing process to balance the activation and outward-diffusion processes. However, the microscopic picture of the doping mechanism is still not clarified. N_O is likely not the only defect type introduced by nitrogen doping. As is well known, when aliovalent substitutions occur in ionic compounds, a charge-compensation mechanism is required to ensure that the overall charge remains neutral. For Cu_2O:N with ionized N_O acceptors, the compensation can be achieved, e.g. through the formation of anion vacancies (V_O) or less likely, cation interstitials (Cu_i) though their formation energy is relatively high[21,22].

Photoluminescence (PL) is a non-destructive technique for the investigation of defects in semiconductors. The PL spectrum of Cu_2O has been adequately researched in the literature, and the luminescence related to excitons, V_O, and V_{Cu} has been well established[24–26]. However, previous research has not produced sufficient results with respect to PL studies of Cu_2O:N. Ishizuka et al. have reported that Cu_2O:N exhibits no PL peak prior to hydrogen or crown-ether cyanide treatment, indicating the existence of non-radiative recombination centers in the polycrystalline Cu_2O[18,19].

Figure 4(a) presents the PL spectra of the Cu_2O samples, with arrows indicating positions related to the excitons, V_O and V_{Cu}. The presence of V_O is due to the oxygen-lean growth conditions. After high-temperature annealing, the exciton luminescence was remarkably enhanced, whereas the intensity of the V_O signature did not change significantly, suggesting an improvement in crystal quality after annealing. Notably, the formation of V_{Cu} was suppressed because of the oxygen-lean conditions during growth, enabling a strong exciton luminescence[25,26]. The shape of the exciton luminescence peak can be well interpreted in terms of phonon-assisted transitions, as discussed in Ref. 26.

Figure 4(b) presents the spectra of the Cu_2O:N films while the spectrum of the Cu_2O sample annealed at 750°C is also included as a reference. The most distinguishable features are the suppressed

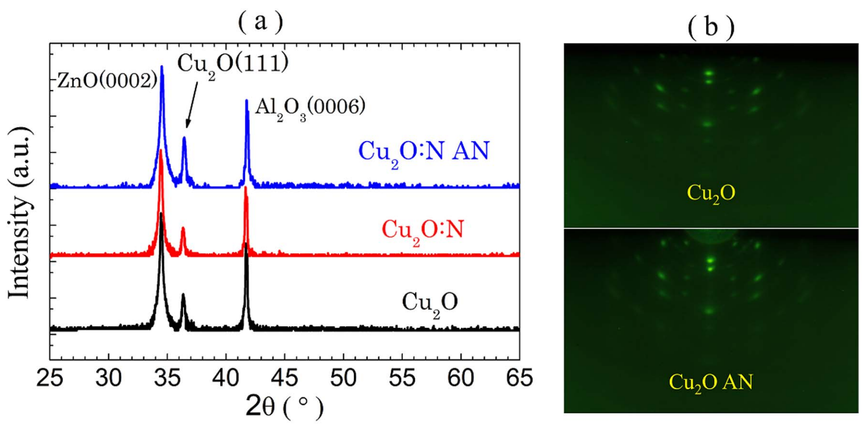

Figure 1 | (a) Typical XRD θ-2θ scans of the samples and (b) in situ RHEED patterns of undoped Cu_2O sample, which are similar to those of Cu_2O:N.

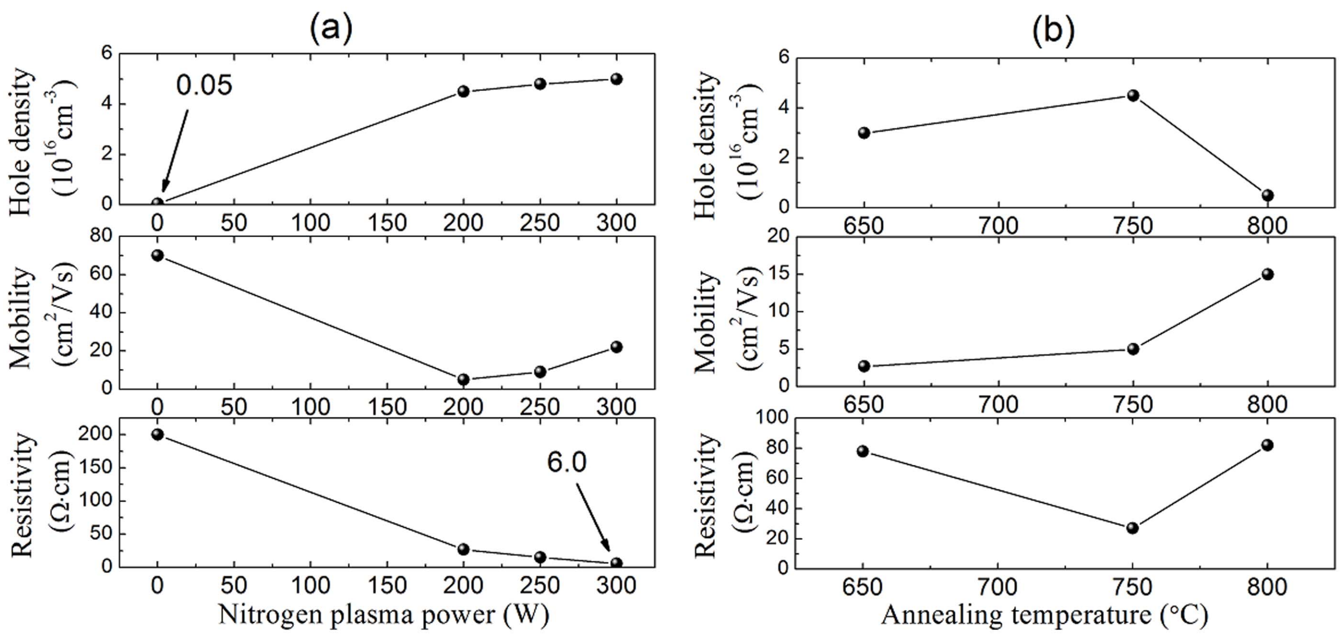

Figure 2 | Hole density, hole mobility, and resistivity of (a) Cu_2O:N samples annealed at 750°C as functions of the nitrogen plasma power (a power of 0 W represents an undoped sample) and (b) Cu_2O:N samples doped with a nitrogen plasma power of 200 W as functions of the annealing temperature.

exciton luminescence and intense V_O–related luminescence of the Cu_2O:N films after annealing, supporting our hypothesis that incorporation of nitrogen is associated with the V_O generation. Concurrently it has been demonstrated that the presence of V_O has no responsibility for damping the exciton luminescence[25,26], suggesting other traps to be involved and specifically N_i and N_O may be considered as prime candidates for non-radiative recombination mechanisms.

Indeed, the exciton luminescence was slightly enhanced (see Fig. 4(c)), whereas the intensity of the V_O signal, in contrast, decreased with increasing annealing temperature. Taking into account the fact that PL intensities are proportional to defect contents, the evolution of the V_O signature suggests that the annealing processes somehow reduced the V_O content in the Cu_2O:N samples. It should be mentioned that the as-grown Cu_2O:N sample is likely to contain the highest density of V_O; however, this fact was not directly reflected by the PL intensity because of the poorer crystallinity of the as-grown sample. Considering that the annealing process played a limited role in repairing the V_O in the undoped Cu_2O (see Fig. 4(a) and Ref. 26), this trend of decreased V_O concentration in Cu_2O:N should be attributed to the evolution of defects not available in the undoped films. A reasonable explanation is the refilling of V_O by interstitial atoms, likely N_i, which move faster at higher temperatures and thus can more easily occupy the vacancy sites. Interstitial oxygen (O_i) is another possible candidate to react with V_O; however, its formation is disfavored under oxygen-lean growth conditions[21,22]. Thus, the difficulty encountered in judging the conduction type of the as-grown Cu_2O:N based on the Hall measurements is the natural result of the presence of less N_O and more N_i in the film.

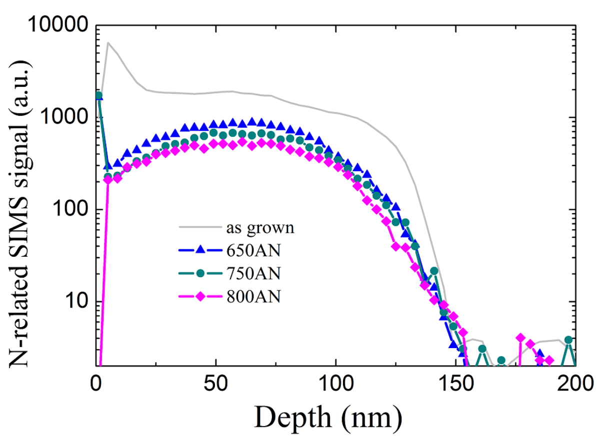

Figure 3 | Nitrogen concentration versus depth profiles in Cu_2O:N samples.

Further evidence for N_i is observed in Figure 4(c), the enlarged spectra of the Cu_2O:N films in the vicinity of the exciton level. The as-grown Cu_2O:N sample exhibited a unique signature located at ~652 nm (1.90 eV). This signal did not originate from the β band in nonstoichiometric Cu_2O, despite the very similar energy level (1.91 eV) because the β band created by exciton-defect complexes would not be affected by the annealing process[27,28]. It cannot be related to N_O; if it were, it would not have disappeared after annealing. Therefore, this 652 nm peak is most likely attributable to the emission related to N_i. The absence of this signature in the annealed samples is the result of the diffusion of nitrogen out of the material and the transformation of N_i into N_O. This interpretation is reasonable, considering the variation in the V_O signature and the electrical properties.

It is worth noting that for all our samples, no signature could be observed at approximately 680 nm (Fig. 4(b)), where Ishizuka et al. observed a lone peak in the PL spectrum of Cu_2O:N after passivation treatment[18,19]. Park et al. have also reported the observation of this 680 nm luminescence signature in Cu_2O films without intentional doping[29], indicating that the origin of this feature in polycrystalline Cu_2O thin films remains uncertain.

In order to extend our interpretation, we applied X-ray photoelectron spectroscopy/X-ray Auger electron spectroscopy (XPS/XAES) to probe the defects[30–32]. A comparative study was conducted using four samples – two as-grown and two 750°C annealed samples of Cu_2O and Cu_2O:N, labeled as Cu_2O, Cu_2O AN, Cu_2O:N, and Cu_2O:N AN, respectively. Notably, the confirmation of the nitrogen atoms' locations from their chemical states or bonding status is impractical because no signal related to nitrogen could be detected because of the low doping level (~10^{18} cm^{-3}). Instead, we relied on

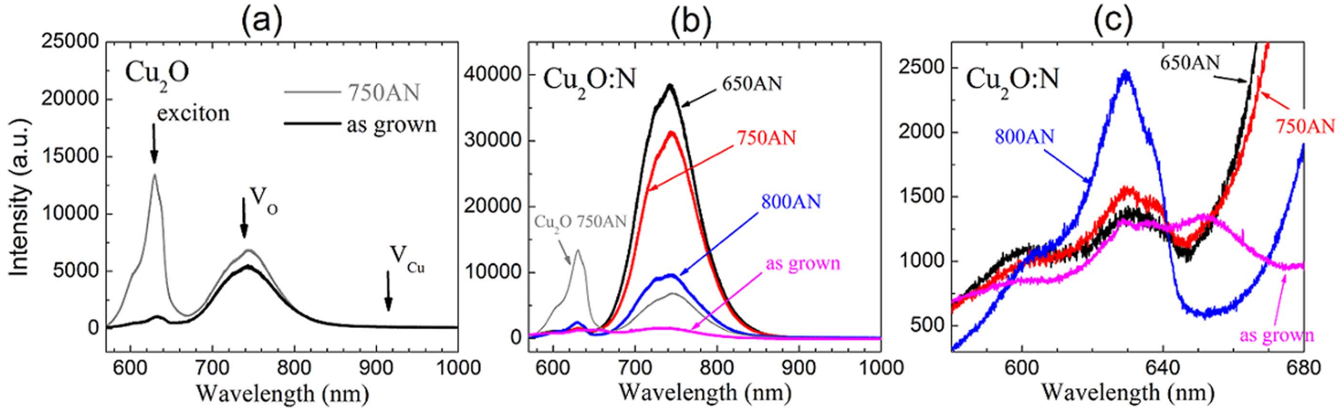

Figure 4 | Photoluminescence spectra of (a) Cu_2O samples, (b) Cu_2O:N samples doped at 200 W, and (c) enlarged portion of (b) in the vicinity of the exciton emission.

the detection of other defects to interpret the formation and evolution of nitrogen-related defects by means of the defects' interactions.

Figure 5 presents the high-resolution XPS spectra of the (a) Cu2p and (b) O1s core levels. As shown in Fig. 5(a), the Cu-related peaks exhibit a symmetric shape with no satellite structure at approximately 943 eV, ruling out the presence of Cu^{2+} in these films. The fitting of the Cu2p3/2 peaks indicates a binding energy of 932.6 eV, corresponding to that of Cu^{+} in Cu_2O. The presence of metallic Cu clusters may also be ruled out accounting for: (i) the Cu2p peaks exhibit strong symmetry, and the full widths at half maximum (FWHM) for all different samples are nearly identical (1.43–1.49 eV); (ii) the XRD results show no evidence of Cu (Fig. 1); and (iii) the samples exhibited good p-type conductivity. Further, the signatures of the O1s peaks at 530.4 eV are consistent with O-state in Cu_2O too. Notably, a much more pronounced variation in the FWHM values (1.15–1.58 eV, see Fig. 5(b)) indicates a trend that may be correlated with the presence of V_O based on literature interpretations of oxygen deficient samples[30,31].

As XAES is much more sensitive to the nature of the neighboring bonds and/or point defects than XPS[30,32], the evolution of Cu LMM Auger lines was measured and Fig. 6 shows typical Cu-related signatures deconvoluted with five different components. Notably, three peaks located at 913.5 eV, 919.5 eV and 921.4 eV are known not to be sensitive to the chemical environment[33–35]. The dominating peaks in Fig. 6 at 916.8 eV (labeled as peak 1) and 918.3 eV (labeled as peak 2) are typically attribute to Cu_2O and Cu, respectively, though peak 2 can also be observed in nonstoichiometric Cu_2O[33,34]. In fact, the appearance of peak 2 in Fig. 6 is intriguing since we have ruled out the presence of Cu_i or Cu cluster in our films. An alternative identification of peak 2 may be to assign it to V_O, since strong localized unpaired electrons of copper atoms neighboring V_O might influence its effective charge state readily detectable by XAES[21,22,30]. In another words, the signal of Cu next to V_O (-O-Cu-V_O-), i.e. Cu dangling bond, is distinguishable from Cu^{1+} (-O-Cu-O-), assuming that one V_O would lead to an "aggregation" of four Cu atoms (Fig. S3 in the supplementary information).

Adopting this identification, further conclusions may be done considering the evolution of the peaks intensities in Fig. 6. Notably, the annealing results in much more pronounced decrease of the V_O content (in terms of the integrated intensity ratio of peak1 and peak 2) in Cu_2O:N, comparing to that in Cu_2O, which is consistent with the PL results, altogether suggesting a critical role of N_i to interact with V_O in the course of annealing. Indeed, during annealing, the supply of atmospheric oxygen is insufficient to change V_O concentration drastically, while the presence of N_i in Cu_2O:N makes the major contribution to interact with V_O forming N_O.

The higher ratio of the annealed Cu_2O:N sample indicates the lower V_O content, i.e., fewer Cu dangling bonds, compared with the annealed Cu_2O sample; this finding reflects the important influence of the growth conditions, as the nitrogen plasma provided additional total anions. One may argue that this result seems to be in conflict with the stronger V_O-related luminescence of Cu_2O:N, as shown in Figure 5(b). We attribute this phenomenon to the passivation effect of nitrogen[36], which arises because N_i can also move to defect sites other than V_O. This passivation effect is further evidence of significant N_i formation induced by doping. Ishizuka et al. also observed an enhanced PL intensity after nitrogen doping[18].

Notably, the fitted FWHMs of peak 1 for the Cu_2O:N samples (Table 1) are slightly broadened compared with those of the undoped Cu_2O samples. Fixing the FWHMs of peak 1 yielded very similar

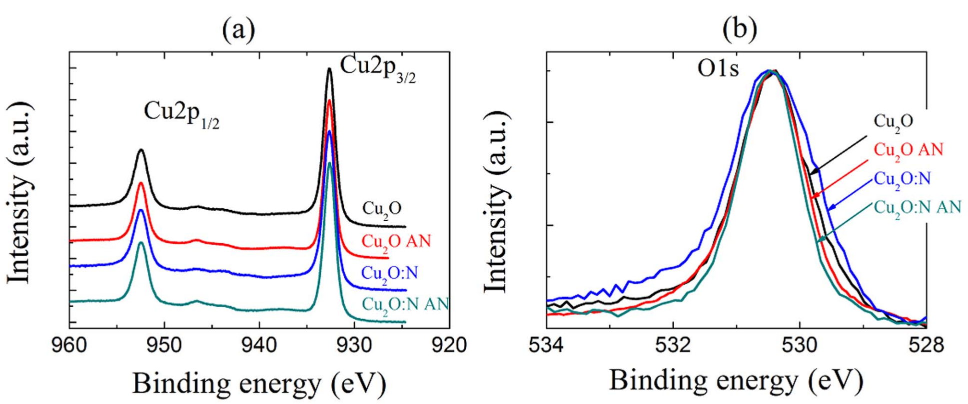

Figure 5 | XPS (a) Cu 2p spectra, and (b) normalized O 1s spectra of Cu_2O and Cu_2O:N samples.

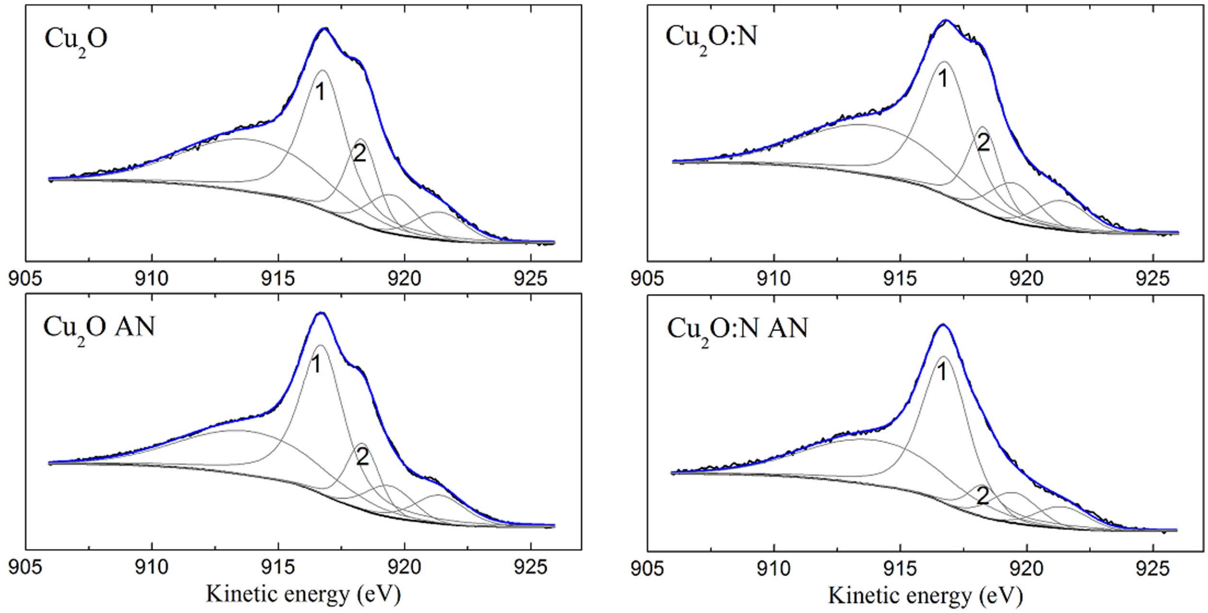

Figure 6 | Cu LMM spectra demonstrated with 5 different components for the Cu_2O (left column) and Cu_2O:N (right column).

fitting results; however, it was found that allowing this broadening improved the fit considerably, yielding a smaller standard deviation. This broadening is interpreted as a sensitive indication of Cu-N bonding, as supported by the Cu LMM spectrum of a Cu_3N thin film, which exhibits a similar shape to that of Cu_2O, also with a predominant peak at 916.8 eV (supplementary information).

In conclusion, Cu_2O and Cu_2O:N thin films were synthesized through the oxidation of Cu films. N_O acceptors effectively enhance the conductivity of such films, with an activation energy of approximately 121 meV. Probing the defects in the films using a combination of PL and XPS/XAES revealed the formation of N_i and the enhancement of the V_O content in the prepared Cu_2O:N thin films. The evolution of the optical and electrical properties of these films can be consistently explained in terms of the N_i interacting with V_O and the resultant transformation into N_O in the course of annealing.

Methods

The samples were fabricated in an ultra-high-vacuum chamber with a background pressure within the lower range of 10^{-7} Pa. A conventional Knudsen cell was used to evaporate metallic Cu (6N). Cu (111) films were initially deposited on c-plane Al_2O_3 buffered with a 400 nm thick semi-insulating ZnO (0001) film. Cu_2O films were obtained via post-oxidation using oxygen plasma, and Cu_2O:N films were obtained under similar conditions through co-treatment with oxygen and nitrogen plasmas. Specifically, the oxygen plasma was used at a fixed O_2 flux of 1 sccm (the partial pressure was maintained within the lower range of 10^{-3} Pa), and discharged via RF power. The doping level was controlled by varying the RF power and the N_2 flux. The thickness of the prepared films was approximately 150 nm. The oxidation/doping temperature was 300°C for all samples. The typical oxidation time was approximately 90 minutes. The oxidation process was monitored by means of in situ reflection high-energy electron diffraction (RHEED) observations. Once the RHEED pattern indicated complete oxidation of Cu into Cu_2O, the plasma exposure was terminated.

Table 1 | Summary of the Cu LMM peak-fitting parameters

Sample	Peak	K.E. [eV]	Intensity	FWHM [eV]	Intensity ratio
Cu_2O	1	916.8	19252.42	2.10	2.56
	2	918.3	7519.22	1.52	
Cu_2O AN	1	916.7	22386.87	2.10	3.61
	2	918.3	6193.66	1.52	
Cu_2O:N	1	916.8	12843.29	2.30	2.43
	2	918.3	5276.19	1.52	
Cu_2O:N AN	1	916.8	18128.31	2.20	6.83
	2	918.3	2655.39	1.52	

Shorter or longer treatment times would result in undesired phases of Cu and CuO, respectively. More details can be found in our previous report[20].

Several samples were subjected to post-annealing in the same chamber under an oxygen-gas atmosphere (also at ~10^{-3} Pa) at various temperatures. The temperature ramping rate was 30°C min^{-1}. Once the set temperature was reached, that temperature was maintained for 10 min, and the sample was then cooled at the same rate of 30°C min^{-1}.

XRD measurements were performed using a Mac Science M18XHF diffractometer with a Cu Kα radiation source (λ = 1.5406 Å) at 40 kV and 50 mA (2 kW).

The van der Pauw configuration was used for the Hall measurements. Room-temperature tests were performed using an Ecopia HMS-3000 system, and the results were double-checked using a home-made Hall system. The Hall coefficient was extracted from the trace curve of the transverse voltage recorded using an alternating magnetic field and a constant current (supplementary information). The temperature-dependent hole density was recorded using a Lakeshore model 7604 Hall system. The acceptor level was extracted using the following equation:

$$p=\frac{N_A-N_D}{2N_D}N_v\exp\left(\frac{-E_A}{kT}\right) \tag{1}$$

where N_A, N_D, N_v, E_A, k and T are the acceptor density, donor density, effective density of states in the valence band, acceptor level, Boltzmann constant, and absolute temperature, respectively, and

$$N_v=2(2\pi m_h kT/h)^{3/2} \tag{2}$$

where m_h and h are the hole effective mass and the Plank constant, respectively.

For the photoluminescence measurements, the samples were excited using a 532 nm laser at 1 mW focused to a spot of approximately 2 μm. The spectra were measured at room temperature in a back-scattering geometry. The integration time was 10 seconds in all cases.

SIMS measurements were performed using a Cameca IMS 7f microanalyzer.

XPS measurements were performed using a PHI-5300 ESCA Spectrometer with a monochromatic Al k_α X-ray source at 1486.6 eV. All data were collected at a nominal depth of 6 nm after Ar-ion sputtering, and the damage effect proved to be negligible (supplementary information). Spectral analysis was performed using XPSPeak version 4.1. Shirley background subtraction was adopted, and the fitting results were determined based on the minimum standard deviation.

1. Hara, M. *et al.* Cu_2O as a photocatalyst for overall water splitting under visible light irradiation. *Chem. Commun.* **3**, 357–358 (1998).
2. Hu, C.-C., Nian, J.-N. & Teng, H. Electrodeposited p-type Cu_2O as photocatalyst for H_2 evolution from water reduction in the presence of WO_3. *Sol. Energy Mater. Sol. Cells* **92**, 1071–1076 (2008).
3. Kuo, C.-H., Yang, Y.-C., Gwo, S. & Huang, M. H. Facet-Dependent and Au Nanocrystal-Enhanced Electrical and Photocatalytic Properties of Au-Cu_2O Core-Shell Heterostructures. *J. Am. Chem. Soc.* **133**, 1052–1057 (2011).
4. Huang, W.-C., Lyu, L.-M., Yang, Y.-C. & Huang, M. H. Synthesis of Cu_2O Nanocrystals from Cubic to Rhombic Dodecahedral Structures and Their Comparative Photocatalytic Activity. *J. Am. Chem. Soc.* **134**, 1261–1267 (2012).

5. Kalidindi, S. B., Sanyal, U. & Jagirdar, B. R. Nanostructured Cu and Cu@Cu_2O core shell catalysts for hydrogen generation from ammonia–borane. *Phys. Chem. Chem. Phys.* **10**, 5870–5874 (2008).
6. Malerba, C. *et al.* Nitrogen doped Cu_2O: A possible material for intermediate band solar cells? *Sol. Energy Mater. Sol. Cells* **105**, 192–195 (2012).
7. Lee, Y. S. *et al.* Nitrogen-doped cuprous oxide as a p-type hole-transporting layer in thin-film solar cells. *Mater. Chem. A* **1**, 15416–15422 (2013).
8. Luque, A. & Martí, A. Increasing the Efficiency of Ideal Solar Cells by Photon Induced Transitions at Intermediate Levels. *Phys. Rev. Lett.* **78**, 5014–5017 (1997).
9. Diwald, O. *et al.* Photochemical Activity of Nitrogen-Doped Rutile TiO_2(110) in Visible Light. *J. Phys. Chem. B* **108**, 6004–6008 (2004).
10. Valentin, C. D., Pacchioni, G., Selloni, A., Livraghi, S. & Giamello, E. Characterization of Paramagnetic Species in N-Doped TiO2 Powders by EPR Spectroscopy and DFT Calculations. *J. Phys. Chem. B* **109**, 11414–11419 (2005).
11. Kudo, A. & Miseki, Y. Heterogeneous photocatalyst materials for water splitting. *Chem. Soc. Rev.* **38**, 253–278 (2009).
12. Lai, G., Wu, Y., Lin, L., Qu, Y. & Lai, F. Low resistivity of N-doped Cu_2O thin films deposited by rf-magnetron sputtering. *Appl. Surf. Sci.* **285B**, 755–758 (2013).
13. Zang, Z., Nakamura, A. & Temmyo, J. Nitrogen doping in cuprous oxide films synthesized by radical oxidation at low temperature. *J. Mater. Lett.* **92**, 188–191 (2013).
14. Nakano, Y., Saeki, S. & Morikawa, T. Optical bandgap widening of p-type Cu_2O films by nitrogen doping. *Appl. Phys. Lett.* **94**, 022111 (2009).
15. Li, M., Zhang, J.-Y., Zhang, Y. & Wang, T.-M. Oxygen vacancy in N-doped Cu_2O crystals: A density functional theory study. *Chin. Phys. B* **21**, 087301 (2012).
16. Zhao. *et al.* First-principles study on the doping effects of nitrogen on the electronic structure and optical properties of Cu_2O. *RSC Adv.* **3**, 84–90 (2013).
17. Ishizuka, S., Kato, S., Maruyama, T. & Akimoto, K. Nitrogen Doping into Cu_2O Thin Films Deposited by Reactive Radio-Frequency Magnetron Sputtering. *Jpn. J. Appl. Phys.* **40**, 2765–2768 (2001).
18. Ishizuka, S., Kato, S., Okamoto, Y. & Akimoto, K. Hydrogen treatment for polycrystalline nitrogen-doped Cu_2O thin film. *J. Cryst. Growth* **237–239**, 616–620 (2002).
19. Okamoto, Y. *et al.* Passivation of defects in nitrogen-doped polycrystalline Cu_2O thin films by crown-ether cyanide treatment. *Appl. Phys. Lett.* **82**, 1060–1062 (2003).
20. Li, J. *et al.* Temperature dependence of Cu_2O orientations in oxidation of Cu (111)/ZnO (0001) by oxygen plasma. *Chin. Phys. B* **21**, 076401 (2012).
21. Raebiger, H., Lany, S. & Zunger, A. Origins of the p -type nature and cation deficiency in Cu_2O and related materials. *Phys. Rev. B* **76**, 045209 (2007).
22. Soon, A., Cui, X.-Y., Delley, B., Wei, S.-H. & Stampfl, C. Native defect-induced multifarious magnetism in nonstoichiometric cuprous oxide: First-principles study of bulk and surface properties of $Cu_{2-\delta}O$. *Phys. Rev. B* **79**, 035205 (2009).
23. Paul, G. K., Nawa, Y., Sato, H., Sakurai, T. & Akimoto, K. Defects in Cu_2O studied by deep level transient spectroscopy. *Appl. Phys. Lett.* **88**, 141901 (2006).
24. Itoh, T. & Narita, S. Relaxed excitons in Cu_2O. *J. Phys. Soc. Jpn.* **39**, 132–139 (1975).
25. Ito, T. & Masumi, T. Detailed examination of relaxation processes of excitons in photoluminescence spectra of Cu_2O. *J. Phys. Soc. Jpn.* **66**, 2185–2193 (1997).
26. Li, J. *et al.* Engineering of optically defect free Cu_2O enabling exciton luminescence at room temperature. *Opt. Mater. Express* **3**, 2072–2077 (2013).
27. Zouaghi, M. Near infrared optical and photoelectric properties of Cu_2O II. Near infrared Photoconductivity in Cu_2O: Influence of annealing. *phys. stat. sol. (a)* **11**, 219–227 (1972).
28. Zouaghi, M. Near infrared optical and photoelectric properties of $C_{u2}O$ III. Interpretation of experimental results. *phys. stat. sol. (a)* **11**, 449–460 (1972).
29. Park, J.-W. *et al.* Microstructure, optical property, and electronic band structure of cuprous oxide thin films. *J. Appl. Phys.* **110**, 103503–103508 (2011).
30. Göpel, W. *et al.* Surface defects of TiO_2(110): a combined XPS, XAES and ELS study. *Surf. Sci.* **139**, 333–346 (1984).
31. Fan, J. C. C. & Goodenough, J. B. X-ray photoemission spectroscopy studies of Sn-doped indium-oxide films. *J. Appl. Phys.* **48**, 3524–3531 (1977).
32. Schwidtal, K. SiO_2 Surface defect centers studied by AES. *Surf. Sci.* **77**, 523–536 (1978).
33. Platzman, I., Brener, R., Haick, H. & Tannenbaum, R. Oxidation of Polycrystalline Copper Thin Films at Ambient Conditions. *J. Phys. Chem. C* **112**, 1101–1108 (2008).
34. Poulston, S., Parlett, P. M., Stone, P. & Bowker, M. Surface Oxidation and Reduction of CuO and Cu_2O Studied Using XPS and XAES. *Surf. Interface Anal.* **24**, 811–820 (1996).
35. Antonides, E., Jose, E. C. & Sewatzky, G. A. LMM Auger spectra of Cu, Zn, Ga, and Ge. I. Transition probabilities, term splittings, and effective Coulomb interaction. *Phys. Rev. B* **15**, 1669–1679 (1977).
36. Chobpattana, V. *et al.* Nitrogen-passivated dielectric-InGaAs interfaces with sub-nm equivalent oxide thickness and low interface trap densities. *Appl. Phys. Lett.* **102**, 022907 (2013).

Acknowledgments

The authors would like to thank Prof. Rexi Kui and Prof. Jia-ou Wang for valuable discussions. This work was supported by the Ministry of Science and Technology of China (Grant Nos. 2011CB302002 and 2011CB302006), the National Science Foundation of China (Grant Nos. 11174348, 51272280, 11274366, 61204067, and 61306011), the Chinese Academy of Sciences, and the Research Council of Norway in the framework of the IDEAS grant program administered via the ENERGIX program.

Author contributions

Z.M., Q.M. and X.D. conceived and guided the study. J.L. and Z.M. designed the research and guided the work and analysis. J.L., H.L., L.L. and Y.L. conducted the growth and characterization of the Cu_2O. A.J. conducted the growth and characterization of the Cu_3N. A.A. and A.K. performed the SIMS experiments. J.L. and A.K. wrote the paper. All authors discussed the results and commented on the manuscript.

Additional information

Supplementary information accompanies this paper at http://www.nature.com/scientificreports

Competing financial interests: The authors declare no competing financial interests.

How to cite this article: Li, J. *et al.* Probing Defects in Nitrogen-Doped Cu_2O. *Sci. Rep.* **4**, 7240; DOI:10.1038/srep07240 (2014).